



**HAL**  
open science

## Influence of irradiation parameters on the polymerization of ceramic reactive suspensions for stereolithography

Thierry Chartier, Cyrielle Dupas, Pierre-Marie Geffroy, Vincent Pateloup, Maggy Colas, Julie Cornette, Sophie Guillemet-Fritsch

### ► To cite this version:

Thierry Chartier, Cyrielle Dupas, Pierre-Marie Geffroy, Vincent Pateloup, Maggy Colas, et al.. Influence of irradiation parameters on the polymerization of ceramic reactive suspensions for stereolithography. *Journal of the European Ceramic Society*, 2017, 37 (15), pp.4431-4436. 10.1016/j.jeurceramsoc.2017.05.050 . hal-01727624

**HAL Id: hal-01727624**

**<https://unilim.hal.science/hal-01727624>**

Submitted on 9 Dec 2019

**HAL** is a multi-disciplinary open access archive for the deposit and dissemination of scientific research documents, whether they are published or not. The documents may come from teaching and research institutions in France or abroad, or from public or private research centers.

L'archive ouverte pluridisciplinaire **HAL**, est destinée au dépôt et à la diffusion de documents scientifiques de niveau recherche, publiés ou non, émanant des établissements d'enseignement et de recherche français ou étrangers, des laboratoires publics ou privés.




## Open Archive Toulouse Archive Ouverte (OATAO)

OATAO is an open access repository that collects the work of Toulouse researchers and makes it freely available over the web where possible

This is an author's version published in: <http://oatao.univ-toulouse.fr/24494>

**Official URL:** <https://doi.org/10.1016/j.jeurceramsoc.2017.05.050>

### **To cite this version:**

Chartier, Thierry and Dupas, Cyrielle and Geffroy, Pierre-Marie and Pateloup, Vincent and Colas, Maggy and Cornette, Julie and Guillemet, Sophie   
*Influence of irradiation parameters on the polymerization of ceramic reactive suspensions for stereolithography.* (2017) Journal of the European Ceramic Society, 37 (15). 4431-4436. ISSN 0955-2219

Any correspondence concerning this service should be sent to the repository administrator: [tech-oatao@listes-diff.inp-toulouse.fr](mailto:tech-oatao@listes-diff.inp-toulouse.fr)

# Influence of irradiation parameters on the polymerization of ceramic reactive suspensions for stereolithography

Thierry Chartier<sup>a,\*</sup>, Cyrielle Dupas<sup>a</sup>, Pierre-Marie Geffroy<sup>a</sup>, Vincent Pateloup<sup>a</sup>,  
Maggy Colas<sup>a</sup>, Julie Cornette<sup>a</sup>, Sophie Guillemet-Fritsch<sup>b</sup>

<sup>a</sup> SPTS, Univ. Limoges, CNRS, UMR 7315, F-87000 Limoges, France

<sup>b</sup> CIRIMAT, Univ. Toulouse, CNRS, UPS, F-31062 Toulouse, France

## ARTICLE INFO

### Keywords:

Additive manufacturing  
Stereolithography  
Polymerization  
Irradiation parameters  
Raman spectroscopy

## ABSTRACT

Stereolithography is an additive manufacturing process which makes it possible to fabricate useful complex 3D ceramic parts, with a high dimensional resolution and a good surface finish. Stereolithography is based on the selective UV polymerization of a reactive system consisting in a dispersion of ceramic particles in a curable monomer/oligomer resin. In order to reach a homogeneous polymerization in the green part, and to limit the risk of cracking and/or deformation during subsequent stages of debinding and sintering due to internal stresses, the influence of various fabrication parameters (laser power, scanning speed, number of irradiations) on the degree of polymerization was investigated. In addition, the impact of the irradiation of the subsequent upper layers onto the previously deposited and irradiated layers was evaluated. The degree of conversion was determined by Fourier Transform Infrared Spectroscopy (FTIR). Raman spectroscopy was also used and a brief comparison between these two methods is given.

## 1. Introduction

Conventional ceramic processing routes are limited to the creation of complex shapes and are costly thanks to tooling and/or machining for the fabrication of prototypes or short-range production. Previously called Solid Freeform Fabrication (SFF) or Rapid Prototyping, additive manufacturing (AM) techniques, that open the possibility to produce parts of nearly any shape, are becoming more and more accessible.

AM technologies have shown a growing interest these past few years. At first, simple tools to build polymer prototypes, with the main objective to help for designing parts, AM technologies have become nowadays real production tools, able to shape different materials (polymer, metal, and ceramics) into complex parts. Used in a wide range of industries, AM allows companies to turn innovative ideas into successful end products rapidly and efficiently. In the domain of ceramics, AM technologies constitute an attractive answer to the need of shaping techniques to produce useful complex parts and specific architectures without costly tooling and/or machining. Additive processes are likely going to transform the

field of ceramic manufacturing and will open new ways of thinking about the design and fabrication of objects [1–3].

Among the AM techniques used to fabricate ceramic parts, stereolithography (SLA) is an efficient way to fabricate useful complex 3D objects, with a high dimensional resolution and a good surface finish. Stereolithography is based on the selective UV polymerization of a reactive system consisting of a dispersion of ceramic particles in a curable monomer/oligomer resin with the addition of a photoinitiator [4–7]. Using the three dimensional CAD file of the part to be built, the UV laser beam, focused onto the surface, is deflected in the X-Y plane to polymerize each cross sectional patterns of successive layers of the part to build the 3D green object. The green part is cleaned to remove the remaining non polymerized suspension/paste, then debinded and sintered.

Polymerization is a critical step to control in the stereolithography process. Submitted to UV light, the photoinitiator releases reactive radicals, initiating the polymerization which transforms the liquid monomer/oligomer into solid polymer. In this respect, the manufacture, using stereolithography, of useful complex 3D parts with a high dimensional accuracy and properties similar to those obtained by classical routes requires the understanding of the main process parameters which influence the polymerization. For instance, the higher the degree of conversion of the curable system, the higher the mechanical strength of the green part [8].

\* Corresponding author.

E-mail address: [thierry.chartier@unilim.fr](mailto:thierry.chartier@unilim.fr) (T. Chartier).

It is then critical to determine not only the degree of conversion of the monomer/oligomer system, but also the kinetics of the polymerization, i) to have a pertinent choice of the organic system in terms of kinetics and reactivity, ii) to evaluate the effects of additives such as dispersant and diluent and, iii) to determine the best fabrication parameters such as the layer thickness, the density of energy, the power of the laser, the scanning speed or the number of scans to build a cohesive ceramic green part, without deformation or cracking, in a reasonable time [9,10].

This study considers the last point, based on the determination of the degree of polymerization, with the objective to reach a homogeneous polymerization in the volume of the green sample in order to minimize internal stresses, then the risk of cracking and/or deformation during subsequent stages of debinding and sintering.

Fourier Transform Infrared Spectroscopy (FTIR) is a common method used to determine the final degree of conversion of monomers and oligomers in the polymer industry [11]. Thanks to the absorption band (e.g. acrylate double bond stretching in acrylate resins) area being proportional to the bond concentration, it is possible to follow the evolution of the polymerization, also allowing kinetic studies using Real-Time Infra-Red spectroscopy (RTIR). Several studies of ceramic loaded systems have been performed by FTIR, RTIR [12,13]. Raman spectroscopy has been mainly used to characterize the structural evolution of monomer/oligomer. Nevertheless, Raman spectroscopy is an attractive method to follow the polymerization of a reactive system directly during the fabrication by stereolithography and makes it possible to adjust the manufacturing parameters in real time [14–16].

In this work, the degree of conversion of stereolithography reactive suspensions containing 50 vol% alumina particles submitted to UV laser beam was measured by FTIR and Raman spectroscopies. Then, a comparison of the degree of polymerisation of curable suspensions measured by FTIR and Raman spectroscopies is also presented in this paper. The Raman spectroscopy presents the advantage of being able to be used *in operando*, whereas it is not possible for FTIR for technical constraints. Indeed, the Raman head can be offset by a distance of 15 cm or more from the working plan, which leaves room for the spreading and insulation systems.

## 2. Experimental procedure

### 2.1. Preparation of the alumina reactive system

Stereolithography suspensions are basically composed of a curable oligomer/monomer, a photoinitiator, a ceramic powder and a dispersant. The main requirements for this reactive system are: i) a high powder loading (i.e. >50 vol.%) to ensure suitable mechanical properties to the green part during debinding and a sufficient densification during sintering, ii) a rheological behavior adapted to the spreading of thin layers, i.e. shear thinning and, iii) a sufficient reactivity to UV, even for a concentrated suspension, in order to reduce the time of fabrication with a sufficient cure depth.

The organic media is a mixture of two different reactive resins chosen in the family of acrylates: 1,6-hexanediol diacrylate (HDDA) which is a di-functional monomer (viscosity 25 °C: 7 mPa s) and a tetra-acrylate (PPTTA) with a functionality of 4 (viscosity 25 °C: 190 mPa s). The ratio between the two resins is 10% PPTTA/90% HDDA. The combination of these two resins constitutes a good compromise between high reactivity and low viscosity. The photoinitiator is a 2,2-dimethoxy-1,2-phenylethan-1-one (DMPA) (BASF, Germany), which absorbs in the range of 220–380 nm. Alumina powder P172SB (Alteo, France) has been used (mean particle size: 0.5 μm, specific surface area: 7.6 m<sup>2</sup>/g, density: 3.96 g cm<sup>-3</sup>).

The alumina powder was mixed with the organic media to reach a 50%vol powder loading, with the help of a dispersant, and ball

milled for 4 h. The final suspension is homogeneous and presents a shear-thinning behaviour. The viscosity at 100 s<sup>-1</sup> (25 °C) is 3 Pa s which is in agreement with the layer spreading requirements. A critical energy of 491 mJ cm<sup>-2</sup> has been experimentally determined thanks to the Jacobs equation [4]. The critical energy represents the minimum of energy for which polymerization occurs, and thus describes for the reactivity of the system.

### 2.2. Manufacturing

Thin layers of suspension were spread by means of a moving blade, similar to tape-casting. The thickness of the layers was fixed at 50 μm according to the reactivity of the suspension and in order to reach a good dimensional resolution of the future 3D objects manufactured.

Three types of samples were prepared in order to evaluate, i) the number of layers with a given thickness influenced by the irradiation (A samples), ii) the respective contribution of the scanning speed and of the laser power, at constant density of energy, on the degree of polymerization (B samples) and, iii) the influence of the number of irradiations maintaining a constant density of energy (C samples).

The optical system of the stereolithography machine consists of different elements (Fig. 1):

- a UV laser source with a 355 nm wavelength,
- a laser beam expander which maximises the use of the scan system aperture and reduces the power density on the mirrors,
- a scan head composed of two galvanometer movable mirrors which deflect the laser beam with a high precision and repeatability,
- a F-Theta objective that focuses the laser beam at the focal point. This objective ensures that the focal point is always positioned in the working plane, perpendicular to the optical axis of the objective. The spot size of the laser beam, focused onto the surface, has a diameter of 21,6 μm.

#### A-samples

A first objective was to determine the number of layers, with a typical thickness of 50 μm, influenced by the laser irradiation. The upper side of the multilayer object will only be submitted to one irradiation at a given density of energy. Depending on the depth of penetration of the UV light, the layers below can be affected with an increase of their degree of polymerization. In this respect, multilayered samples containing from 2 to 12 layers with a thickness of 50 μm were fabricated. A first 50 μm thick layer was deposited on the working platform and a rectangle zone of 12 × 5 mm<sup>2</sup> was irradiated with an UV laser beam (355 nm), at a constant energy dose (DE = 1.02 J cm<sup>-2</sup>). After moving down the working platform of the layer thickness, a second 50 μm thick layer was deposited on the first one and a same rectangle was irradiated with the same energy dose and so on. The degree of polymerization of the two accessible sides (bottom side and upper side, the upper side being the irradiated side submitted to only one irradiation) was measured.

#### B-samples

The degree of polymerization is directly related to the density of energy DE (J cm<sup>-2</sup>) delivered. We have considered the average density of energy which depends on the spot size of the laser beam radius ω<sub>0</sub> (cm), the scanning speed v<sub>s</sub> (cm/s) and the power of the laser P<sub>0</sub> (W) according to Eq. (1).

$$DE = \frac{2P_0}{\pi\omega_0 v_s} \quad (1)$$

This equation considers the Gaussian distribution of the energy of the laser beam with a radius ω<sub>0</sub> corresponding to a decrease of power of 1/e<sup>2</sup>. The generally named spot size is equal to 2ω<sub>0</sub> [4].

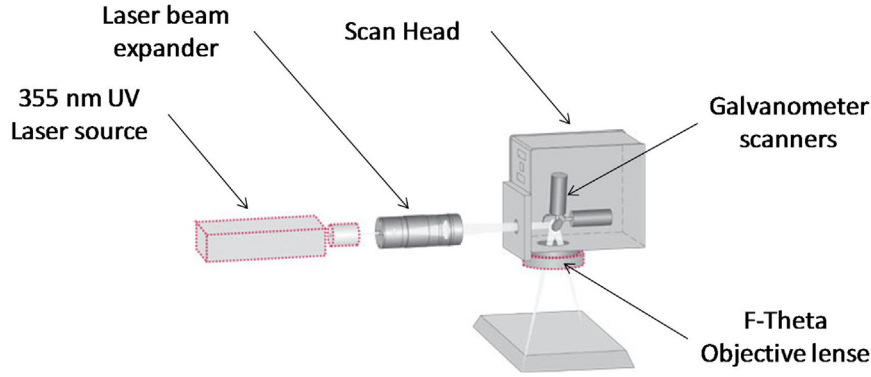


Fig. 1. Schematics of the optical system of the stereolithography machine.

Table 1

Process parameters used to build the B samples ( $DE = 2.55 \text{ J cm}^{-2}$ ).

Sample	Power of the laser (W)	Scanning speed ( $\text{cm s}^{-1}$ )
B-1	0.260	51.0
B-2	0.400	78.4
B-3	0.510	100.0

Table 2

Process parameters used to build the C samples.

Sample	DE per irradiation ( $\text{J cm}^{-2}$ )	Number of irradiations	Total DE received ( $\text{J cm}^{-2}$ )
C-1-a	5.10	1	5.10
C-1-b	2.55	2	5.10
C-2-a	10.20	1	10.20
C-2-b	2.55	4	10.20

Knowing this parameter, the average irradiation of each point of the working surface can be calculated by Eq. (2):

$$H_{average} = \frac{P_0}{\pi \omega_0^2} \quad (2)$$

Considering the time  $t_e$  of exposition of one point by the laser beam given by Eq. (3):

$$t_e = \frac{2\omega_0}{v_s} \quad (3)$$

the average density of energy DE is obtained by multiplying the average irradiation  $H_{average}$  by the irradiation time  $t_e$  (Eq. (1)).

A second objective was to evaluate the respective contribution of the scanning speed  $v_s$  and of the power of the laser  $P_0$ , at constant density of energy, on the degree of polymerization.

For that purpose, rectangular samples ( $12 \times 5 \text{ mm}^2$ ) were fabricated by insulation of a thick layer ( $500 \mu\text{m}$ ) at a constant energy dose ( $DE = 2.55 \text{ J cm}^{-2}$ ) but with different laser power/scanning speed couples. The cohesive polymerized sample was removed, cleaned and characterised (Table 1).

#### C-samples

The third objective was here to evaluate the influence of the number of laser irradiations maintaining a constant density of energy. Rectangular samples ( $12 \times 5 \text{ mm}^2$ ) with a large thickness ( $500 \mu\text{m}$ ), were irradiated one time at a constant energy dose (i.e.  $5.10$  and  $10.20 \text{ J cm}^{-2}$ ) and others received the same total energy dose but with several irradiations at a lower energy dose (Table 2).

#### 2.3. FTIR

The degrees of conversion were calculated from the analysis of infrared spectra obtained using a Nicolet 6700 spectrometer

in attenuated total reflection (ATR). The sample was placed onto the ATR diamond and maintained with a sample holder. The results presented are the average of three measurements made on each surface, each one being an average of 32 scans, with a resolution of  $4 \text{ cm}^{-1}$ . The acrylate double bond absorbance peak at  $1636 \text{ cm}^{-1}$  was monitored. A reference absorption band at  $1720 \text{ cm}^{-1}$ , assigned to the carbonyl group that is not influenced by the polymerization reaction, was also used for the calculation. The degree of conversion of the polymer was calculated as follows (Eq. (4)):

$$C_{FTIR} (\%) = \frac{\frac{A_0^{1620}}{A_0^{1750}} - \frac{A_{end}^{1620}}{A_{end}^{1750}}}{\frac{A_0^{1620}}{A_0^{1750}}} \times 100 \quad (4)$$

with  $A_0$  the peak area measured on the suspension before any UV exposure, and  $A_{end}$  the area measured on the cured sample. The area  $A^{1620}$  corresponds to the area measured in the  $1600\text{--}1650 \text{ cm}^{-1}$  region, while the area  $A^{1750}$  corresponds to the area measured in the  $1650\text{--}1780 \text{ cm}^{-1}$  region.

#### 2.4. Raman

The Raman spectroscopy measurements were performed with a Renishaw Invia Reflex spectrometer at the  $532 \text{ nm}$  wavelength, focused on the surface of the sample using a  $\times 50\text{LDW}$  objective. The laser power on the sample is  $3 \text{ mW}$  over an  $80 \mu\text{m}^2$  surface (line-focus mode). This spectrometer provides a high spectral resolution ( $1.2 \text{ cm}^{-1}$ ). For each spectrum, a baseline correction was applied. As in the case of the FTIR method, normalization of the band of acrylate double bond at  $1636 \text{ cm}^{-1}$  to a reference band was made. The  $1720 \text{ cm}^{-1}$  band corresponding to the carbonyl group stretching was used as the reference. The degree of conversion  $C_{Raman}(\%)$  was calculated using Eq. (5), thanks to the area of the Raman band, obtained by a Lorentzian function decomposition.

$$C_{Raman} (\%) = \frac{\frac{A_0^{1620}}{A_0^{1750}} - \frac{A_{end}^{1620}}{A_{end}^{1750}}}{\frac{A_0^{1620}}{A_0^{1750}}} \times 100 \quad (5)$$

with  $A_0$  the area measured on the suspension before any UV exposure, and  $A_{end}$  the area measured on the cured sample. The area  $A^{1620}$  corresponds to the area measured in the  $1600\text{--}1650 \text{ cm}^{-1}$  region, while the area  $A^{1750}$  corresponds to the area measured in the  $1650\text{--}1780 \text{ cm}^{-1}$  region.

### 3. Results and discussion

#### 3.1. Number of layers (50 μm) affected by the irradiation (DE = 1.02 J cm<sup>-2</sup>) (A-samples)

Fig. 2 shows the degree of conversion obtained by FTIR on the upper side (only one irradiation) and on bottom side which can be influenced by the subsequent irradiations of the upper side. A first comment is the constant conversion of the upper side (about 35%) for all the samples, which demonstrates the repeatability of the effect of a constant density of energy on the conversion rate, the upper side being submitted to only one irradiation.

A second comment concerns the influence of the irradiations of the subsequent layers on the conversion rate of the previously polymerized layers, then the total thickness influenced by the irradiation. The degree of conversion of the bottom side is increasing to reach a level of 67% for the sample 5. For samples 1–5, the irradiation of the upper layer has an effect on the first deposited layer (slice 1).

Using an energy density of 1.02 J cm<sup>-2</sup>, the UV laser initiates the polymerization reaction through 5 layers for our ceramic reactive suspension.

For a thickness larger than 250 μm (5 layers), the difference of conversion between the two sides of the sample is rather constant with a value of about 35%. This difference of polymerisation can induce internal stresses inside the green part, which can lead to cracking and/or deformation during subsequent stages such as debinding and sintering.

The cure depth of a line can be predicted by a beer lambert law [17]:

$$C_d = D_p \ln \frac{DE}{DE_c} \quad (6)$$

The depth of penetration  $D_p$  and the critical density of energy  $DE_c$  (minimum energy for which the polymerisation occurs) are constant characteristics of the suspension. The density of energy  $E$  is supplied by the laser beam.  $D_p$  and  $E_c$  can be calculated by measuring the cure depth of lines polymerised with different densities of energy.

Due to the hatching of the surface during the irradiation, the density of energy is larger than the density of energy delivered for one line ( $DE=1.02 \text{ J cm}^{-2}$  in our case). Considering the hatching space of 20 μm used and a zone of influence of the laser equal to  $2.146(2\omega_0)$  (i.e. 46 μm), a point of the surface is irradiated four times [4].

A new estimation of the average irradiation of the surface, depending on the hatching space  $D_{\text{hatching}}$ , has then to be considered (Eq. (7)) [4]:

$$DE_{\text{surface}} = \frac{P_0}{D_{\text{hatching}} v_s} = 1.73 \text{ J.cm}^{-2} \quad (7)$$

Using the experimental values of  $D_p$  and  $E_c$  (i.e. 103 μm and 0.19 J cm<sup>-2</sup>, respectively), the depth of a cured line calculated using Eq. (7) is 227 μm. This value is in agreement with the fact that the irradiation of the surface layer influences approximately the 4 layers below.

#### 3.2. Influence of the scanning speed $v_s$ and of the power of the laser $P_0$ , at constant density of energy ( $DE = 2.55 \text{ J cm}^{-2}$ ), on the degree of polymerization

Each B sample has received the same energy dose ( $DE=2.55 \text{ J cm}^{-2}$ ) but using different powers of the laser and scanning speeds (Table 1). Even though the energy dose remains constant, the degree of conversion was influenced by laser parameters (power and speed) (Table 3). The higher the power of the

**Table 3**

B-samples degrees of conversion and difference between sample sides ( $DE=2.55 \text{ J cm}^{-2}$ ).

Sample	Degree of conversion (%) Bottom side	Degree of conversion (%) Upper side	Difference between sides
B-1	33	40	7
B-2	34	42	8
B-3	38	47	9

**Table 4**

C-samples degrees of conversion and difference between sample sides.

Sample	Degree of conversion (%) Bottom side	Degree of conversion (%) Upper side	Difference between sides
C-1-a	42	48	6
C-1-b	48	49	1
C-2-a	53	61	8
C-2-b	60	63	3

laser and the quicker the scanning speed are (sample B-3), the larger the difference of degree of conversion between both sides of the sample is.

In order to reach a more homogeneous polymerization, then to decrease the risk of deformation or cracking, a low scanning speed associated to a limited power of the laser seems to be favourable. However, such parameters will increase the building time of the part.

One explanation lies in how the power of the laser is adjusted. Indeed, the power can only be changed by varying the pulse frequency of the source and then, consequently the power of each pulse. In this respect, the frequency of the laser source is higher for the sample B-1 (i.e. lower power of each pulse) than for the sample B-3 (i.e. higher power of each pulse).

The more the irradiance ( $\text{W cm}^{-2}$ ) of the light source is, the more the degree of conversion increases [18]. As the exposure time used in our process is very short, and as the degree of conversion is very dependant of the irradiance for short exposure time at the beginning of the polymerization, it can be considered that the irradiance and then, the power of the light source, influences the degree of conversion.

#### 3.3. Influence of the number of irradiations maintaining a constant density of energy, on the degree of polymerization

Couples of samples C1a/C1b, and C2a/C2b have received the same final density of energy, respectively 5.10 and 10.20 J cm<sup>-2</sup>, but using different numbers of irradiations (Table 2). At constant total density of energy, the number of scans influenced the degree of conversion (Table 4). Sample C-1-a received one UV curing, with an energy dose of 5.10 J cm<sup>-2</sup>. The difference of degree of conversion between the two sides of the sample is 6%. The sample C-1-b received the same energy dose but using two UV irradiations with a lower energy dose, i.e. 2.55 J cm<sup>-2</sup>. The degrees of conversion of the upper sides are similar (48–49%) but the degree of conversion of the bottom side of the sample receiving two irradiations (C-1-b) is larger, reducing the difference of polymerisation through the two faces of the sample down to 1%. With such a low difference, the sample C-1-b can be considered as being homogeneously polymerised.

The same behaviour was observed using a higher final density of energy to increase mechanical properties of the green part. Sample C-2-a received a single curing with an energy dose of 10.2 J cm<sup>-2</sup>, while sample C-2-b received the same total energy dose but in four irradiations of a lower energy dose (2.55 J cm<sup>-2</sup>). The degree of conversion of these samples is logically higher than that obtained for

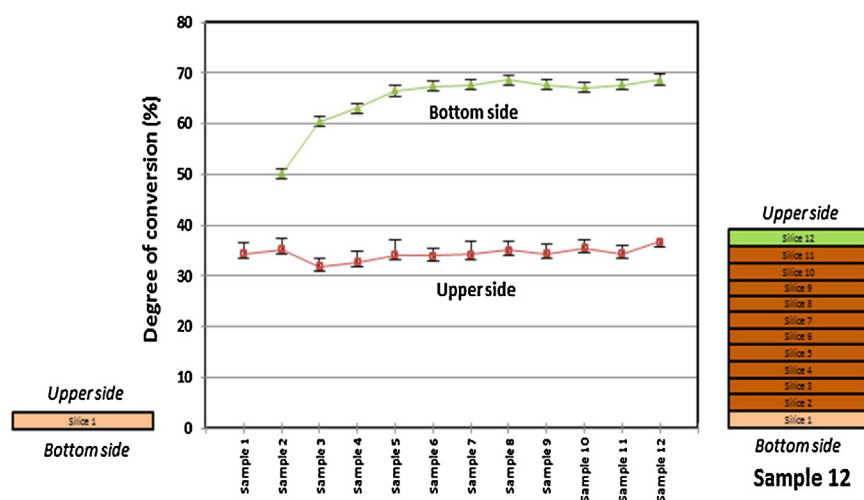


Fig. 2. Degree of conversion on bottom and upper sides of multi-layer samples obtained from FTIR measurements ( $DE = 1.02 \text{ J cm}^{-2}$ ).

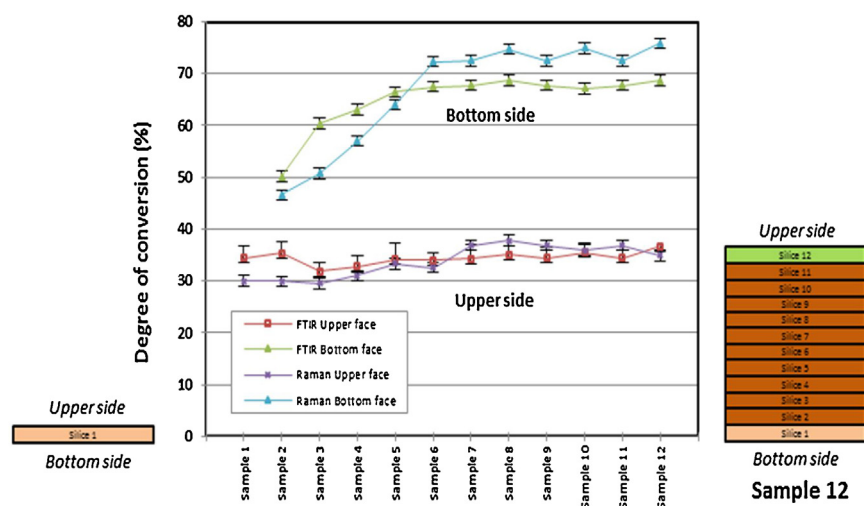


Fig. 3. Degree of conversion on bottom and upper sides of multi-layer samples obtained from both Raman (green) and FTIR (red) measurements ( $DE = 1.02 \text{ J cm}^{-2}$ ). (For interpretation of the references to color in this figure legend, the reader is referred to the web version of this article.)

C-1 samples. The difference of polymerisation between both sides was reduced from 8% (1 scan) to 3% (4 scans).

It is then beneficial to apply the total density of energy in many scans in order to reach a more homogeneous polymerization.

The lower degree of conversion on the bottom side of samples submitted to a high density of energy in one scan (C-1-a and C-2-a) can be explained by the gel effect. The polymerization of the intergranular organic curable phase involves the mobility of reactive radicals released by the photoinitiator submitted to the UV light which lead to the transformation a the liquid monomer/oligomer into a viscous phase (gelation), then into a solid [9,10,19].

The irradiation of the upper side submitted to a high density of energy (C-1-a and C-2-a) will lead to a quick gelation of the surface, then to a lower mobility of reactive radicals, and reduces the degree of conversion of the bottom side. Many irradiations of the upper side with a lower density of energy (C-1-b and C-2-b) maintain a larger mobility of reactive radicals in depth.

With the objective to develop in situ measurements of the degree of polymerization and then to adjust in real time fabrication parameters, Raman spectra for A-samples were recorded (Fig. 3).

The degree of conversion of upper the sides measured by the two methods is similar and rather constant, around 35%. The evolution

of the degree of conversion of bottom sides of multilayer samples is also similar for the two methods of characterisation.

The at-line Raman spectrophotometer could be implemented using a lens instead of an objective to get an average structural response of the material as a function of the external parameters. This lens will unfocus the laser beam, and lead to a larger surface of analysis.

The difference of values of conversion measured by FTIR and by Raman (up to 10%) can be attributed to the size difference of the surface analysed: Raman spectroscopy analyses a surface close to  $80 \mu\text{ m}^2$ , whereas in the FTIR spectroscopy set-up, the area of the analysed surface corresponds to the ATR diamond surface i.e.  $1.76 \cdot 10^6 \mu\text{ m}^2$ . The depth penetration is quite equivalent in the two spectroscopic methods (around  $2 \mu\text{ m}$ ). So the degrees of conversion calculated from FTIR data are averaged from a larger analysis zone.

In addition, the calculation of the area of the bands to evaluate the conversion degree is also different. In the case of Raman, the areas are those of the Lorentzian used to fit the bands while in the case of FTIR, the area used are the integrated intensities of the experimental bands.

The values determined by the two methods are different but follow the same variation. The Raman analysis is more precise in this

case. The at-line Raman spectrophotometer could be implemented using a lens instead of an objective to get an average structural response of the material as a function of the external parameters. This lens leads to a larger surface of analysis but moreover facilitates the implementation of the Raman head in the stereolithography machine since the focal length is 15 cm or more.

#### 4. Conclusions

The influence of various processing parameters in the stereolithography fabrication method (laser power, scanning speed, number of irradiations) on the degree of polymerization was investigated. In addition, the difference of degree of polymerization between the two sides of a green part was evaluated according to the previous processing parameters and to the number of layers influenced by the irradiation of the subsequent layers.

The objective was to reach a homogeneous polymerization in the volume of the green sample in order to minimize internal stresses and hence the risk of cracking and/or deformation during subsequent stages of debinding and sintering.

For a constant density of energy, firstly, a low scanning speed associated to a limited power of the laser and secondly, a multi-curing strategy applying a reduced density of energy in each scan, are both favourable to reach a homogeneous polymerization.

Depending on the thickness of the layers, several layers can be affected by the irradiation of the subsequent upper layers, which may lead to a significant difference of conversion between the two sides of the green part. In the example of our ceramic curable system and using a density of energy of  $1.02 \text{ J cm}^{-2}$ , the UV laser continues the polymerization reaction through five  $50 \mu\text{m}$  thick layers previously irradiated. Thanks to first Raman results, a Raman spectrophotometer will be implemented on the stereolithography fabrication machine to control in situ the degree and kinetics of polymerization and then to be able to adjust in real time fabrication parameters.

#### Acknowledgement

A part of this work was supported by the Agence Nationale de la Recherche under the TERAMETADIEL convention (grant ANR-12-BS03-0009).

#### References

- [1] T. Chartier, A. Badev, Rapid Prototyping of Ceramics, in: S. Somiya, M. Kanen (Eds.), In Handbook of Advanced Ceramics, Second Edition, 2013.
- [2] J. Dekers, J. Vleugels, J.-P. Kruth, Additive manufacturing of ceramics: a review, *J. Ceram. Sci. Technol.* 05 (04) (2014) 245–260.
- [3] A. Zocca, P. Colombo, C.M. Gomes, J. Günster, Additive manufacturing of ceramics: issues, potentialities and opportunities, *J. Am. Ceram. Soc.* 98 (7) (2015) 1983–2001.
- [4] P. Jacobs, Rapid Prototyping & Manufacturing: Fundamentals of Stereolithography, Society of manufacturing Engineers, Dearborn (MI), 1992.
- [5] G. Brady, J. Halloran, Stereolithography of ceramic suspensions, *Rapid Prototyp. J.* 3 (1997) 61–65.
- [6] C. Hinczewski, S. Corbel, T. Chartier, Ceramic suspensions suitable for stereolithography, *J. Eur. Ceram. Soc.* 18 (1998) 582–590.
- [7] T. Chartier, C. Dupas, M. Lagorceix, J. Brie, C. Champion, N. Delhote, C. Chaput, Additive manufacturing to produce complex 3D ceramic parts, *J. Ceram. Sci. Technol.* 06 (2) (2015) 95–104.
- [8] C.-J. Bae, J. Halloran, Influence of residual monomer on cracking in ceramics fabricated by stereolithography, *Int. J. Appl. Ceram. Technol.* 8 (6) (2011) 1289–1295.
- [9] A. Badev, Y. Abouliatim, T. Chartier, L. Lecamp, P. Lebaudy, C. Chaput, C. Delage, Photopolymerization kinetics of a polyether acrylate in the presence of ceramic fillers used in stereolithography, *J. Photochem. Photobiol. A-Chem.* 222 (1) (2011) 117–122.
- [10] T. Chartier, A. Badev, Y. Abouliatim, P. Lebaudy, L. Lecamp, Stereolithography process: influence of the rheology of silica suspensions and of the medium on polymerization kinetics – cured depth, *J. Eur. Ceram. Soc.* 32 (2012) 1625–1634.
- [11] T. Scherzer, U. Decker, Real time FTIR-ATR spectroscopy to study the kinetics of ultrafast photopolymerization reactions induced by monochromatic UV light, *Vib. Spectrosc.* 19 (2) (1999) 385–398.
- [12] K. Wu, J. Halloran, Photopolymerization monitoring of ceramic stereolithography resins by FTIR methods, *J. Mater. Sci.* 40 (2005) 71–76.
- [13] J. Halloran, V. Tomeckova, S. Gentry, S. Das, P. Cilino, et al., Photopolymerization of powder suspension for shaping ceramics, *J. Eur. Ceram. Soc.* 31 (2011) 2613–2619.
- [14] H. Edwards, A. Johnson, I. Lewis, Applications of Raman spectroscopy to the study of polymers and polymerization processes, *J. Raman Spectrosc.* 24 (1993) 475–483.
- [15] N. Brun, I. Youssef, M.-C. Chevrel, et al., In situ monitoring of styrene polymerization using Raman spectroscopy. multi-scale approach of homogeneous and heterogeneous polymerization processes, *J. Raman Spectrosc.* 44 (2013) 909–915.
- [16] S. Khalil, M. Allam, W. Tawfik, Use of FT-Raman Spectroscopy to determine the degree of polymerization of dental composite resin cured with a new light source, *Eur. J. Dentistry* 1 (2007) 72–79.
- [17] S.P. Gentry, J.W. Halloran, Depth and width of cured lines in photopolymerizable ceramic suspensions, *J. Eur. Ceram. Soc.* 33–10 (2013) 1981–1988.
- [18] F. Courtecuisse, F. Karasua, X. Allonasa, C. Croutxé-Barghorna, L. van der Ven, Confocal Raman microscopy study of several factors known to influence the oxygen inhibition of acrylate photopolymerization under LED, *Prog. Org. Coat.* 92 (2016) 1–7.
- [19] A. Maffezzoli, R. Terzi, Effect of irradiation intensity on the isothermal photopolymerization kinetics of acrylic resins for stereolithography, *Thermochim. Acta* 321 (1998) 111–121.



**Thierry Chartier** is CNRS (National Center for Scientific Research) Research Director and Head, since 2008, of the “Science of Ceramic Processes and Surface Treatments” (SPCTS) Laboratory which bring together staff from CNRS and University of Limoges (<http://www.unilim.fr/spcts/>). The vocation of SPCTS laboratory located in Limoges, France, is the “Understanding and control of the elaboration processes, for ceramic and surface treatments, to produce ceramic components, layers...with specific, improved, reliable properties”. He received an engineers’ degree from ENSCI, and a MSc in Ceramic Materials and Surface Treatments from the Univ. of Limoges (1982). He obtained his Ph.D. degree from the Un. of Limoges in

1985 concerning the relation between elaboration-microstructure and properties of SiAlON. His main research interests are ceramic processing with the understanding of fundamental mechanisms that take place during transformation of the mater and the development of new ceramic shaping methods such as additive technologies in order to elaborate complex ceramic parts. His current research concerns additive manufacturing. T. Chartier is the author/co-author of 170 reviewed papers and 38 patents. He was chairman of the 13th conference of the ECerS held in Limoges in 2013. He is member of the World Academy of Ceramics, Fellow of the European Ceramic Society, member of the French Ceramic Group council. He received the “Chaudron” award from the French Society of Metallurgy and Materials (SF2M) (2011), the JECs Trust Award (2015), the Materials Innovation Medal from the Federation of European Materials Societies (FEMS) (2017).